Journal of JSEM, Vol.10, Special Issue (2010) 119-124

Observation of Cylindrical Surfaces by Laser Microscopy with a Wide Field of View

Isami NITTA[1], Rintaro EBUCHI[1] and Hai HUAN[1]

[1] School of Science and Technology, Niigata University, Niigata 950-2181, Japan

(*Received 8 January 2010; received in revised form 2 May 2010; accepted 12 June 2010*)

Abstract

We have developed a new method for observation of cylindrical surfaces. The cylindrical surfaces were observed using a laser microscope with a wide field of view. When cylindrical specimens are rotated by a motor-driven rotary table, the focused laser light is scanned along a generatrix of the cylinder surface. Thus, the whole cylinder surface can be observed easily even over a very short period. As the obtained image is a developed view of the cylinder surface, it is easy to measure the distance between any two points on the cylindrical surface.

Key words

Shrink Fitter, Laser Microscope, Wide Field of View, Cylindrical Surface, Confocal Microscope

1. Introduction

An optical or scanning electron microscope is usually used to observe object surfaces. However, only a very small fraction of the surface can be observed at a time due to the limitations of the field of view of such microscopes [1]. To obtain an image of the whole object surface to be investigated, large numbers of pictures of adjacent positions must be photographed using a CCD camera through the microscope with the specimen moved in a step-by-step feed operation. These pictures have to be combined with each other to make an image of the whole object surface. Thus, such observations are seldom performed. However, observation of the whole surface will provide a better understanding than examination of only part of the surface. We have been engaged in development of a new type of laser microscope with resolution almost as high as that of optical microscopes but with a much wider field of view.

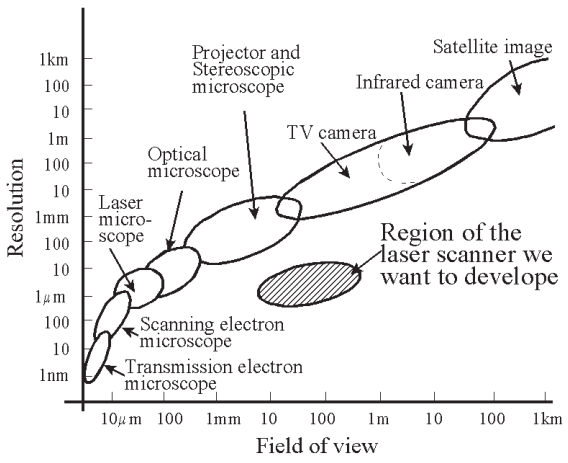

Fig.1 Relationship between resolution and field of view of various microscopes

Figure 1 shows the relationship between the resolutions of various microscopes and their fields of view. With an optical microscope, it is possible to inspect an object on a scale of several tens of micrometers. The same object can be observed on a finer scale with a scanning electron microscope (SEM). However, the field of view of the SEM is narrower than that of the optical microscope. Thus, the field of view narrows as the resolution of the microscope increases. We are currently attempting to develop a new type of laser microscope with resolution as high as that of an optical microscope, but with a much wider field of view.

Figure 2 shows a schematic diagram of the new type of laser microscope. The key technology in this microscope is the scanning lens unit, the fθ lens. It is necessary to focus a laser beam bundle on the object surface, *i.e.*, the focal plane, to a few micrometers over a wide scanning width. Such a fine laser spot can be focused easily on the object surface only at the center of the scanning width, but is

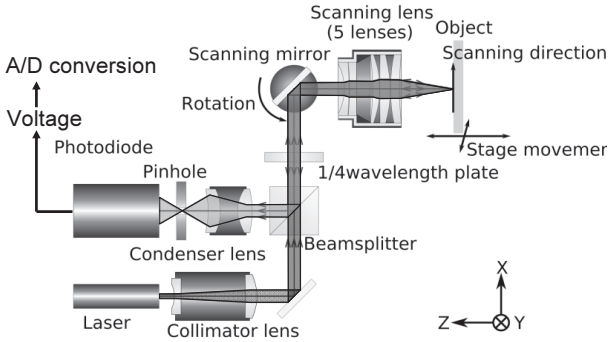

Fig.2 Schematic diagram of the new type of laser microscope

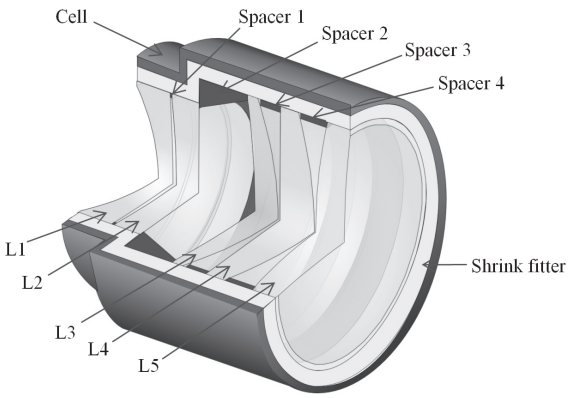

Fig.3 Laser scanner lens with a wide field of view of 50 mm

Table 1 Mechanical properties of each element

Elements	Materials	Young's Modulus [GPa]	Poisson's Ratio	Coefficients of Thermal Expansion [10^{-6} K^{-1}]
L1	Glass	70.8	0.285	9.3
L2	Glass	62.3	0.227	9.0
L3	Glass	121.9	0.291	6.2
L4	Glass	121.9	0.291	6.2
L5	Glass	121.9	0.291	6.2
Shrink fitter	POM	2.8	0.475	100
Housing	Al(A5056B)	69.0	0.340	24.0

difficult at the edges. The poor location of each scanning lens relative to the housing can adversely affect the size and shape of the laser spot on the focal plane, especially near the ends of the scanning width. The optical axes of each lens must be coincident with each other and should not be moved even with changes in room temperature [2].

Here, we report that a shrink fitter, a new machine element developed by one of the authors [3 – 9], greatly improves the performance of the fθ scanning lens. The fitting pressure between the optical lenses and the metallic housing decreases with temperature because their coefficients of thermal expansion differ from each other. However, the shrink fitter could maintain a constant fitting pressure of the shrinkage fit of such a combination despite changes in room temperature.

With this shrink fitter technology, we have already developed a new type of laser microscope with a field of view of 10 × 8 mm as shown in Fig.4 [4]. Here, we attempted to increase the field of view to 50 × 40 mm. The pixel number in the laser scanning direction is 20,000 and that in the perpendicular direction is 16,000. The observation results of some surfaces and also cylindrical surfaces using this laser microscope are described.

2. Shrink Fitter

The shrink fitter is a new machine element of cylindrical geometry, as shown in Fig. 2. When two machine elements with different thermal expansion coefficients are subjected to shrink fitting, the fitting pressure will vary with temperature. However, it is possible to keep the fitting pressure constant using the shrink fitter, even if the circumferential temperature changes. The shrink fitter is connected to a polygonal mirror and a self-acting air bearing [8]. In addition, an assembly with an all-ceramic bearing and a metal housing was also examined to improve the performance of the ceramic bearing using the shrink fitter [10]. In the present study, the shrink fitter was applied to accurately locate the lenses in the housing for a new type of laser microscope with a wide field of view. The cylindrical shrink fitter is made of a plastic material, the Young's modulus of which is lower than that of the metal by about two orders of magnitude. Thus, a larger amount of interference can be used for the shrinkage fit of such a combination. If the room temperature increases, the housing will expand more than the lenses. The interference of the shrinkage fit without use of the shrink fitter will decrease at elevated temperatures. The reduced interference and the gap between the lenses and the housing reduce the performance of the scanning lens. However, the coefficient of thermal expansion of the plastic material is larger than that of the metal. Thus, if the thickness of the shrink fitter is designed appropriately, the interference will not change even at elevated temperatures. Consequently, the contact pressure acting on the lens rim due to the shrinkage fit will remain constant regardless of changes in temperature. Thus, the performance of the scanning lens will not change dependent on temperature.

3. Shrink Fitter Method for a New Laser Microscope: Procedure for Determination of Critical Interference

In the shrink fit method, excessive interference will cause large-scale deformation of fitted lenses, resulting in deterioration of the focusing performance [3]. Therefore,

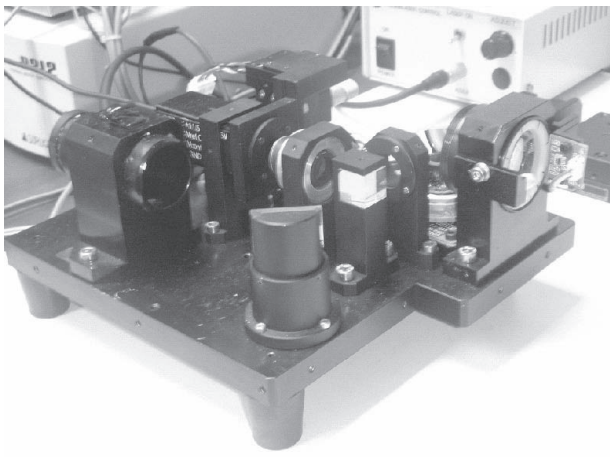

Fig.4 Laser microscope described in a previous paper with a wide field of view of 10 × 8 mm

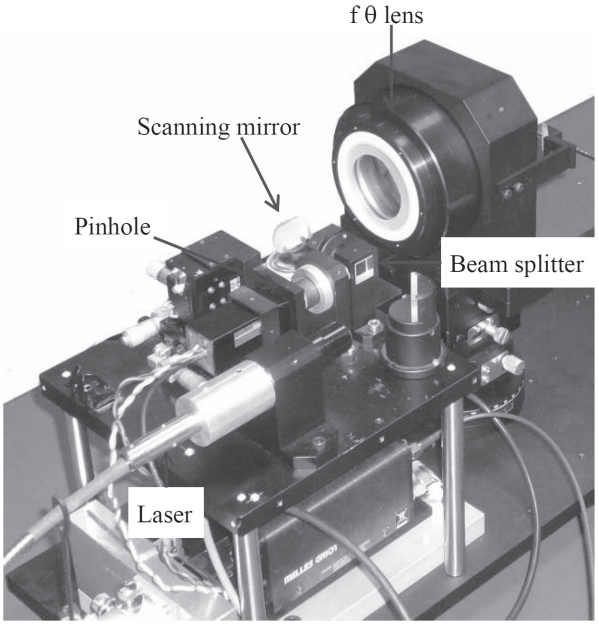

Fig.5 Newly developed laser microscope with a wide field of view of 50 × 40 mm

the critical interference under which the focusing performance is not reduced must be determined for appropriate use of the shrink fit method. A procedure to determine the critical interference is described below along with the laser scanner lens system shown in Fig. 3. The fθ lens shown in Fig. 3 consists of five lenses, designated L1, L2, L3, L4, and L5. These five lenses are shrink-fitted into the aluminum housing by the shrink fitter. A laser beam with a wavelength of 408 nm is irradiated from a laser diode as shown in Fig. 2. The fθ lens is designed such that the laser spot may be kept at a constant diameter of 10 μm over a wide scanning width of 50 mm on the image plane. The mechanical properties of each component are shown in Table 1. Deformation of each lens corresponding to various interferences is calculated in axisymmetric analysis using commercial FEM software, MARC. The laser beam diameters are then simulated using commercial optical design software, CodeV, taking all lens deformations into consideration. Once the allowable interference is obtained, we can assemble the fθ lens by the shrink fitter method without deterioration of the focusing performance if the interference can be kept below the critical value.

The procedure mentioned above is just rigorous one that is used for a very high performance fθ lens. However, in this paper we did not calculate the allowable interferences. And each lens was shrink-fitted with almost zero micrometer interference based on our experience so far.

4. Outline of the Developed Laser Microscope

Figure 2 shows a schematic optical path diagram of the new type of laser microscope developed in this study. First, a laser beam bundle emitted by a laser diode is made as parallel as possible through a collimating lens. In addition, a linearly polarized collimated laser beam is transformed into a circularly polarized beam by a quarter wave plate. The laser beam is scanned by a rotating flat mirror at a rotational speed of 9,000 rpm and passes through the fθ lens unit to focus the laser beam bundle on the focal plane at a laser spot diameter of about 10 μm over a scanning width of 50 mm. The reflected laser beam become

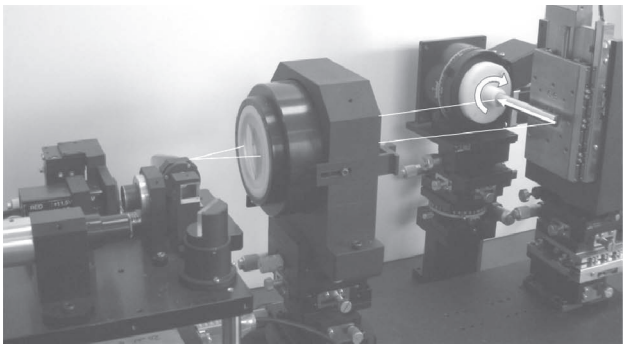

Fig.6 Laser microscope for cylindrical surfaces with a motor-driven rotary stage instead of a linear

polarized at right angles to the outgoing laser beam from the fθ lens unit, which allows good separation at the polarizing beam splitter. Finally, the reflected laser beam passed to a photodetector through a pinhole. The intensity of the reflected laser beam is transformed into digital data by a 12-bit A/D converter at a conversion rate of 100 MHz. The rotating flat mirror scans the laser beam in the horizontal direction and the specimen attached to the motor-driven stage can be moved in the vertical direction at a constant speed controlled by a microcomputer. Thus, the surface of the specimen to be observed can be scanned by the fine laser beam and the image of the surface is produced by arranging the signals of the reflected laser light in the horizontal and vertical directions.

This fθ lens unit has a telecentric property such that the outgoing laser beams from the fθ lens to the specimen to be inspected are parallel to the optical axis of the fθ lens unit. Telecentric lenses yield constant magnification over a range of working distances, virtually eliminating viewing angle error. With telecentric lenses, the image size remains almost unchanged when the object distance changes, provided the object to be inspected remains within the given field depth/telecentric range. In addition, the fθ lens unit must be designed such that the image height is proportional to the scan angle (θ), not the tangent of that

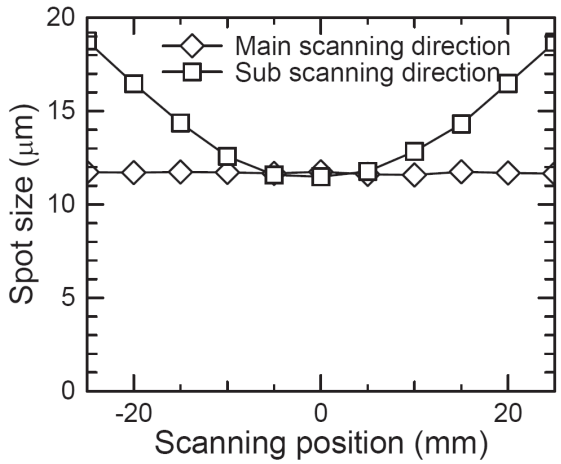

Fig.7 Measured laser spot sizes using a diode laser with a wavelength of 408 nm

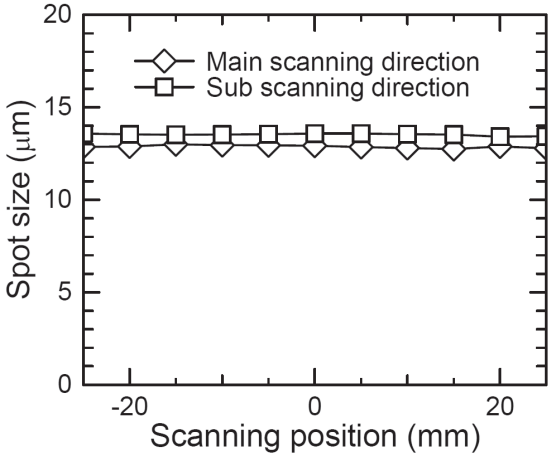

Fig.8 Measured laser spot sizes using a solid-state laser with a wavelength of 408 nm

angle: converting the equiangular motion of the laser beams to the constant speed motion for the scanning operation.

Figure 5 shows a photograph of the new type of laser microscope. As mentioned above, we usually use a motor-driven linear stage moved in the vertical direction to observe flat surfaces. However, use of a motor-driven rotary stage instead of the linear stage, as shown in Fig. 6, facilitates observation of cylindrical surfaces. A whole cylindrical surface can be observed in a relatively short time with this method compared to other techniques. This new laser microscope transforms a cylindrical surface into a developed view.

5. Basic Performance of the Laser Microscope

The laser spot diameters on the focal plane were simulated using the optical design software, Code V. The fθ lens was designed such that the laser spot diameters could be kept at almost a constant value of 10 μm over the whole scanning width. Figure 7 shows the laser spot diameters as a function of scanning position over the scanning width of 50 mm, measured using a SpotScan model 0390 (Photon Inc.). The laser spot sizes at several scanning positions were measured in two different directions: one was in the scanning direction by the rotating flat mirror, main scanning direction, and the other was in the orthogonal direction, sub- (or vice-) scanning direction, as the laser spot emitted from the laser diode is not perfectly circular but slightly elliptical although the laser beam from the laser diode is reshaped into an almost circular spot through two cylindrical lenses before the collimator lens. The laser spots measured at the middle of the scanning width in the main scanning direction were about 12 μm in diameter. The laser spots increased in size as the laser beam was scanned toward both the scanning ends. The laser spot diameter in the main scanning direction is smaller than that in the sub-scanning direction.

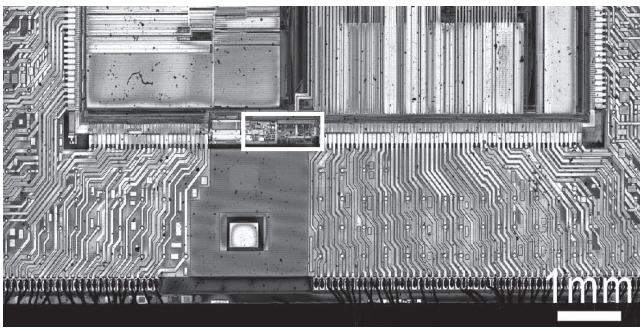

Fig.9 Image of a CPU observed using the developed laser microscope

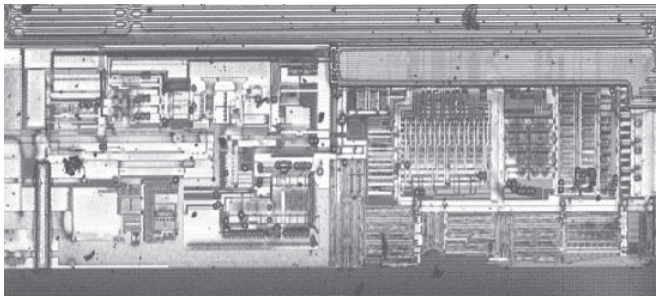

Fig.10 Detailed image of the white rectangular portion in Fig. 9

In the Code V simulation, the laser beam bundle is assumed to have a Gaussian distribution of intensity. Instead of the diode laser of 408 nm a solid-state laser of 488 nm having a Gaussian distribution of intensity is used. Figure 8 shows the measured results of the laser spot sizes on the focal plane. It can be seen that the measured spot sizes in both main and sub directions remained constant over the whole scanning width of 50 mm. These observations indicate that the scanning lens assembled in this study has the designed optical performance. Thus, the 408 nm diode laser does not have a Gaussian distribution of intensity and therefore the spot sizes of the laser beam do not remain constant over the scanning width as shown in Fig. 7.

The resolution of the laser microscope was evaluated using a USAF resolution target, consisting of bars organized into groups and elements (Edmund Optics) [10]. A positive target has only the chrome pattern deposited on the glass substrate, so it had a black pattern with a clear field. Each group consists of six elements (*i.e.*, elements 1 – 6), each of which is composed of three horizontal and three vertical equally spaced bars. Each element within a group corresponds to an associated resolution, based on the bar width/space, in the range from 0.8 μm to 500 μm. The resolution of an imaging system is defined by the group and element just before the black and white bars begin to blend together. The vertical bars are used to calculate horizontal resolution and the horizontal bars are used to calculate vertical resolution. One line pair equals one black and one white bar.

The resolution in the main scanning direction was about 11.0 μm around the middle of the scanning width. It decreased toward both the scanning ends corresponding to the tendency of the laser spot sizes. The resolution in the sub-scanning direction was 24.8, which was worse than that in the main scanning direction corresponding to the laser spot sizes on the focal plane shown in Fig. 7.

6. Images Observed with the Laser Microscope

Figure 9 shows an image of a CPU observed using the laser microscope with a field of view of 10 mm developed in a previous study. The cover of the CPU package for a personal computer was removed and set on the stage of the laser microscope to observe its circuit pattern. The measured area was 10 mm in width and 4 mm in height. The scanning width of 10 mm is a limitation of the fθ lens unit. However, the vertical scanning width of 4 mm is not a limitation inherent to the laser microscope but is dependent on the limitation of the mechanical stage used. Thus, longer surfaces can also be observed.

It is obvious that a huge area can be observed at a time compared with the conventional optical microscope. This laser microscope also has a deep depth-of-focus and therefore the images were very clear despite the rough surface.

The pixel number in the laser scanning direction of 10 mm was 20,000, and thus the distance from pixel to pixel

was 0.5 μm. Figure 9 has a total of 320,000,000 pixels. Thus, any portion in Fig. 9 can be seen at higher magnification. Figure 10 shows a portion of Fig. 9 bounded by the white rectangle on a finer scale; very fine patterns that could not be seen in Fig. 9 were visible.

Figure 11 shows a developed image of a high-carbon Cr steel surface. The shaft diameter is 10 mm and its length is 50 mm. Polishing scars can be seen in the vertical direction. Generally, it is very difficult to measure the length between any two points on a cylindrical surface. However, Fig. 11 shows a developed image of the cylindrical surface and indicates that it is very easy to measure the distance between two points. In addition, the red rectangular area in Fig. 11 can be magnified quite easily because image data at that magnification have already been obtained by the laser microscope.

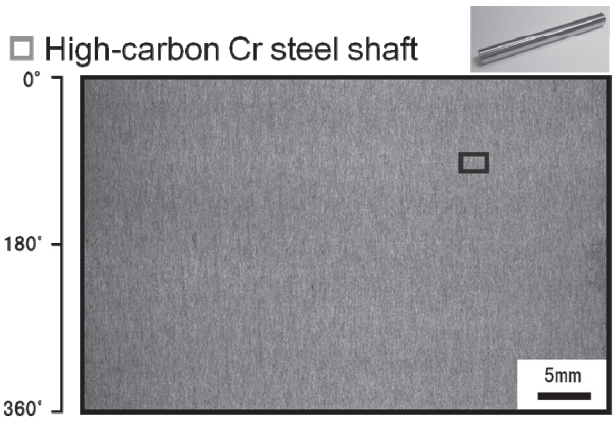

Fig.11 Developed view of a high-carbon Cr steel shaft

Figure 12 shows the magnified image of the red rectangular area in Fig. 11. Several long and short scratched scars can be seen in the horizontal direction. Thus, this type of laser microscope is suitable for inspection of all tiny scars on cylindrical surfaces over a short time scale.

Figure 13 shows a TiN-coated 4-edge end mill 10 mm in diameter. In the end mill cutting process, a variety of grooves, slots, and pockets may be produced in the work piece from a variety of tool bits. Square end cutters can mill square slots, pockets, and edges. Each cutting edge appears as a spiral on the cylindrical surface. However, the cutting edge is a straight line when the cylindrical surface of the end mill is developed. The cylindrical surface of the end mill is very uneven. It is very difficult to focus on the cylindrical surface because of the very large distance

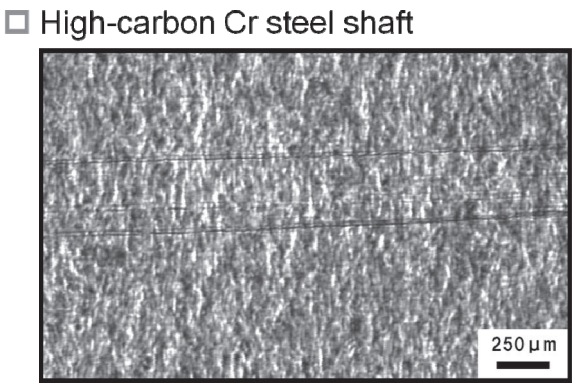

Fig.12 Magnified image of blue rectangular area in Fig. 11

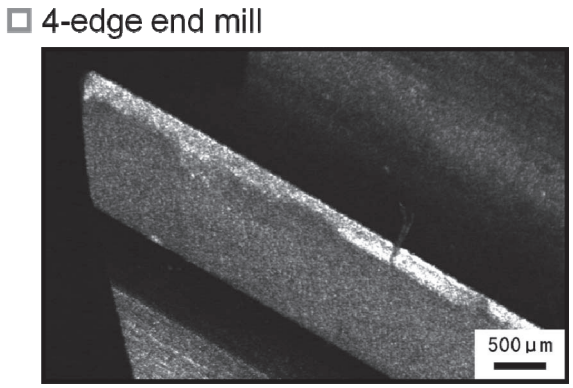

Fig.14 Magnified image of blue rectangular area in Fig. 13

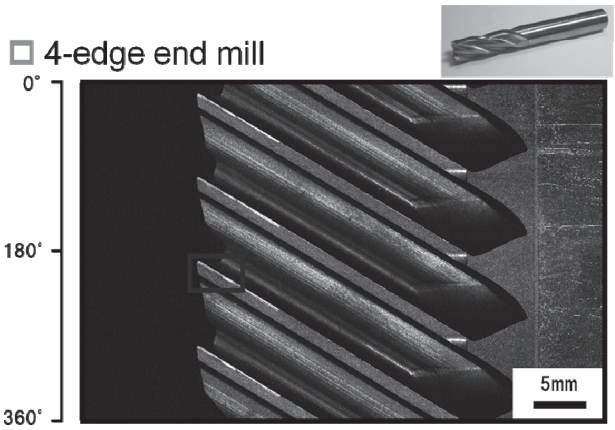

Fig.13 Developed image of a 4-edge end mill

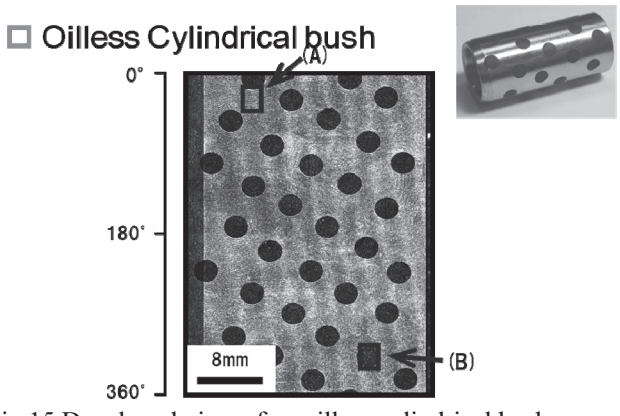

Fig.15 Developed view of an oilless cylindrical bush

between the high and low levels. However, this laser microscope has a deep depth-of-focus so the whole image of the end mill can be obtained simultaneously without additional adjustment of focus. This end mill was used to make a groove on a steel surface. The four cutting edges have wear scars of the same length.

Figure 14 shows a magnified image of the red rectangular area in Fig. 13. The wear scars can be clearly observed. Wear damage was clearly different from point to point, and it was quite easy to obtain measurements of the lengths and widths of the wear scars.

Figure 15 shows the surface of an oilless cylindrical bush. The self-lubricating oilless bushes are graphite embedded type bushes, with holes of equal size and spacing drilled all over the walls to cover approximately 25% of the total surface area. These holes are then plugged with graphite rods acting as solid lubricant, which is constantly available for lubrication during the lifetime of the bush. It can be seen from Fig. 15 that graphite rods are not equispaced because of manufacturing errors. Thus, the laser microscope described here can be used for quality management of the cylindrical products.

Figure 16 shows magnified images of the red rectangular areas in Fig. 15. Due to the holes for embedding of graphite, tool chatter occurs when the cutting tool is bouncing off the part and cutting intermittently rather than cutting continuously. These roughened surfaces may adversely affect lubrication performance of the bush. Generally, it is difficult to observe graphite surfaces because they are black in color and have low reflection rates. However, the new laser microscope can be used to observe graphite surfaces and its surface roughness can be clearly visualized.

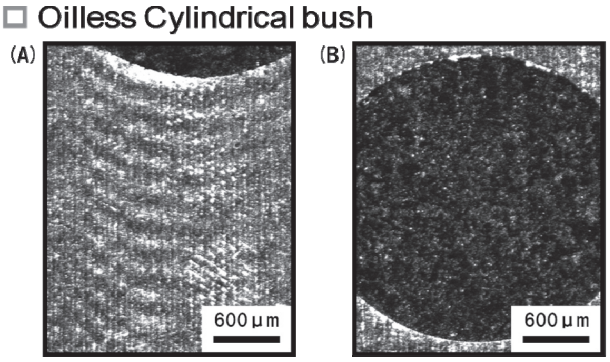

Fig.16 Magnified images of blue rectangular area in Fig. 15

7. Conclusions

Shrink fitter technology has made it possible to shrink fit optical lenses into a given housing without serious reduction of the focusing performance due to changes in room temperature. The procedure to determine the critical interference was described. With the shrink fitter technology, a new type of laser microscope with a large field of view of 10 mm or 50 mm was developed. Several images obtained using this laser microscope were presented. Especially, the cylindrical surface of a steel shaft, the 4-edge end mill, and the oilless bush were closely observed.

Acknowledgments

This work was partially supported by Grant-in-Aid for Scientific Research (B) 21656045 from the Japan Society for the Promotion of Science.

References

[1] Nitta, I., Kanno, A., Komata, K. and Iguchi, S.: New Joining Method for Laser Scanner Lenses by Using a Shrink Fitter, *Proc. 5th Int. Conf. on Computational Methods in Contact Mechanics*, Ed. Dominguez & Brebbia C.A., WIT press (2001), 31-40.

[2] Yoder, P.R.: Opto-Mechanical Systems Design , Third Edition, CRC Press(2005), 202-204.

[3] Nitta, I., Kanno, A. and Komata, K.: Effect of Interference on Scanning Performance of fθ Lens Fixed by a Shrink Fitter, *Optical Review*, **10**-4 (2003), 321-324.

[4] Nitta, I. and Kanno, A. : Contact Problems between Optical Lenses and Shrink Fitter for a New Type of Laser Microscope with a Wide Field of View, *Proc. 8th Int. Conf. on Computational Methods in Contact Mechanics*, Ed. J.T.M.De Hosson, Brebbia C.A. & S-I Nishida, WIT press (2007), 101-110.

[5] Nitta, I., Kigoshi, K. and Kato, K.: Study of the Fitting Strength between Ceramic and Metal Elements with the Use of a Shrink Fitter at Elevated Temperature, *JSME International Journal*, Series III, **32**(1989), 632-639.

[6] Nitta, I., Nakashizuka, K. and Hara, T.: The Fitting Strength between Ceramic and Metal with the Use of a Bimetal Shrink Fitter at Elevated Temperature, *JSME International Journal*, Series I, **34**(1991), 249-256.

[7] Nitta, I., Kusama, K. and Hara, T.: Shrink Fit between a Ceramic and a Metal Element Using a Hybrid Shrink Fitter, *JSME International Journal*, Series C, **38**(1995), 617-624.

[8] Nitta, I., Furukawa, H., Komata, K. and Konno, D.: New Method of Joining a Polygon Mirror Using a Shrink Fitter (in Japanese), *Trans. Jpn. Soc. Mech. Eng*. **62**(1996), 2785-2791.

[9] Nonaka, S., Nitta, I., Kanno, A. and Nishimura, M.: Study of a Laser Material Processing System with Fine Optical Setup using a Shrink Fitter, *Proc. of the Int. Conf. Leading Edge Manufacturing in 21st Century*(2003), 873-877.

[10] Nitta, I., Okamura, A., Shirai, K., Kitamura, K., Takebayashi, H. and Ohashi, O.: Effect of a Shrink Fitter on Load-Carrying Capacity of a Ceramic Bearing at Elevated Temperature (in Japanese), *Trans. Jpn. Soc. Mech. Eng*. **67**(2001), 3291-3297.

[11] EdmundOptics, http://www.edmundoptics.com/techSupport/DisplayArticle.cfm articleid=248.